Mon. Not. R. Astron. Soc. **384,** 1165–1177 (2008) doi:10.1111/j.1365-2966.2007.12794.x

Nekhoroshev stability at L_4 or L_5 in the elliptic-restricted three-body problem – application to Trojan asteroids

Ch. Lhotka,[1⋆] C. Efthymiopoulos[2⋆] and R. Dvorak[1⋆]

[1]*Institute for Astronomy, University of Vienna, Tuerkenschanzstrasse 17, A-1180 Vienna, Austria*
[2]*Research Centre for Astronomy and Applied Mathematics, Academy of Athens, Soranou Efessiou 4, GR-115 27 Athens, Greece*

Accepted 2007 November 27. Received 2007 November 26; in original form 2007 October 19

ABSTRACT

The problem of analytical determination of the stability domain around the points L_4 or L_5 of the Lagrangian equilateral configuration of the three-body problem has served in the literature as a basic celestial mechanical model probing the predictive power of the so-called Nekhoroshev theory of exponential stability in non-linear Hamiltonian dynamical systems. All analytical investigations in this framework have so far been based on the circular restricted three-body problem (CRTBP). In this work, we extend the analytical estimates of *Nekhoroshev stability* in the case of the planar elliptic-restricted three-body problem (ERTBP). To this end, we introduce an explicit symplectic mapping model for the planar ERTBP, obtained via Hadjidemetriou's method, which generalizes the family of mappings discussed in earlier papers. The mapping is based on an expansion of the disturbing function up to a sufficiently high order in the eccentricities and the variations of the semimajor axis, and it is given as a series around a period-one fixed point of the system. Within the domain of the mapping's convergence, we then compute a Birkhoff normal form for 4D symplectic mappings as well as the associated approximate integrals of motion which can be expressed in terms of proper elements. The variations of the integrals predicted by the remainder of the normal form series provide a lower bound for the domain of Nekhoroshev stability for a time at least equal to the age of the Solar System. In the case of Jupiter's Trojans, the domain of the mapping's convergence lies entirely within the region of librational motion, in which the longitude of the perihelion of the asteroid librates around a fixed point value of ϖ. For most asteroids outside this domain macroscopic chaotic diffusion cannot be ruled out. The present analysis provides a physically relevant estimate of the domain of Nekhoroshev stability for proper librations ($D_{\rm p} < 10^0$), and marginal for proper eccentricities ($e_{\rm p} < 0.01$). The formalism is developed in a general way allowing for applications in both, our Solar System and extrasolar system dynamics.

Key words: methods: analytical – celestial mechanics – minor planets, asteroids.

1 INTRODUCTION

The problem of stability of the orbits in a finite region around the equilateral Lagrangian points of the restricted three-body problem has served as a basic probe of the concept of exponential stability in non-linear Hamiltonian systems since Littlewood (1959a,b). Following the initial formulation of Nekhoroshev theorem of exponential stability in non-degenerate Hamiltonian non-linear systems (Nekhoroshev 1977; Benettin, Galgani & Giorgilli 1985), extensions of this theorem were found in the case of isochronous systems with elliptic equilibria (Giorgilli 1988) or isochronous symplectic mappings with elliptic fixed points (Bazzani, Marmi & Turchetti 1990). In the late 90s, the theorem was further generalized by Guzzo, Fassó & Benettin (1998) and Fassó, Guzzo & Benettin (1998) in non-isochronous formulations to systems with elliptic equilibria. In these extended theorems, the small parameter is essentially the distance ρ from the equilibirum (or fixed point), and the theorems assert that orbits librating around the equilibria at a distance ρ (in phase space) have a stable motion for times exponentially long in $1/\rho$, i.e. the following statement holds true:

$$|\rho(t) - \rho(0)| \leq \rho(0)^{\alpha} \; \forall t \leq T_{\rm Nek} = O\left\{ \exp\left[\left(\frac{\rho_*}{\rho} \right)^{b} \right] \right\}. \quad (1)$$

⋆E-mail: christoph.lhotka@univie.ac.at (ChL); lhotka@astro.univie.ac.at (ChL); cefthim@academyofathens.gr (CE); dvorak@astro.univie.ac.at (RD)

Here, α, b are exponents depending on the number of degrees of freedom (d.o.f.) (in isochronous systems with diophantine frequencies, the estimate $b = 1/n$ was given by Giorgilli 1988 that was further improved to $b = 2/n$ in Efthymiopoulos, Giorgilli & Contopoulos 2004). The constant ρ_* is a maximum distance up to which the 'Nekhoroshev regime' applies. If we fix the time of stability $T_{\rm Nek}$, we can solve (1) for ρ and find the maximum distance for which an orbit is guaranteed to be Nekhoroshev stable for at least the time $T_{\rm Nek}$. In Solar System dynamics, we usually set as an upper bound $T_{\rm Nek} \sim 10^{10}$ yr.

Particular applications of the above estimates were given in the case of the Sun–Jupiter–Trojans equilateral configuration: the Trojan asteroids lie in the 1:1 mean motion resonance with Jupiter, and they perform librating motions around Jupiter's L_4 or L_5 points, located at 60° before and after Jupiter on Jupiter's orbit. The libration is asymmetric with respect to the Lagrangian points and the amplitude of libration can reach large values ($\lesssim 35^\circ$), which means that this libration becomes highly non-linear. But even this is only a narrow part of the libration region allowed by the elliptic-restricted three-body problem (ERTBP), which may increase up to $\simeq 75^\circ$ (Érdi 1997).

Nekhoroshev stability estimates in the planar and circular problem were given by Simó (1989), Giorgilli et al. (1989), Celletti & Giorgilli (1991), Giorgilli & Skokos (1997), Efthymiopoulos (2005) and Efthymiopoulos & Sándor (2005). The spatial circular case was treated by Giorgilli et al. (1989) and Skokos & Dokoumetzidis (2001). The applicability of the non-isochronous formulation of Nekhoroshev theory for the Trojan problem was further investigated by Benettin, Fassò & Guzzo (1998). In early applications, the analytical estimated area of stability was extremely small ($\rho \sim 10^4$ km, Celletti & Giorgilli 1991). However, the area calculated by Giorgilli & Skokos (1997), using a computer program to calculate the Birkhoff normal form, was large enough to include some real asteroids. The most recent results of Efthymiopoulos & Sándor (2005), using modified Delaunay variables and a symplectic mapping model of the co-orbital motion, produced a domain of stability in the space of proper elements (Milani 1993) large enough to include 48 per cent of the real asteroids. Of course, this is an overestimate due to the simplification of the circular restricted three-body problem (CRTBP) as the basic model. Nevertheless, such a result indicates that the analytical apparatus of the Nekhoroshev theory can be used to produce estimates which are not only mathematically relevant but also physically relevant.

In this paper, we generalize the formalism developed in previous works (Efthymiopoulos 2005; Efthymiopoulos & Sándor 2005) in order to produce Nekhoroshev estimates for the domain of stability around L_4 or L_5 in the framework of the planar elliptic-restricted three-body model. To this end, we derive an explicit 4D symplectic mapping to represent the motion in Delaunay-like elements yielding the libration of the semimajor axis, critical argument, eccentricity and longitude of the perihelion of the massless body. The stability region is determined as a domain in the space of proper elements (proper libration angle versus proper eccentricity) within which the variations of the proper elements remain bounded for a time exceeding the age of the Solar System. The formalism developed below is quite general and can be used to estimate analytically a domain of stability in all physical cases in which the ERTBP is a good model. In fact, the case of Jupiter's Trojan asteroids, which is motivated by our sample observation of these asteroids, is definitely not the ideal example, since (i) many asteroids have large inclinations, and (ii) the resonant dynamics in this case is affected by practically all the planets of the outer Solar System (Robutel, Gabern & Jorba 2005). Thus, as in all the analytical investigations for these asteroids cited above, the results obtained here should be considered as only indicative of the method. A generalization of the method to include the Nekhoroshev stability of proper inclinations is straightforward. Other cases to which the method lends itself are the equilateral configurations of other planets in our Solar System, or of the major planets of extrasolar planetary systems. Indeed, it has been proposed that terrestrial Trojan planets may exist in some observed extrasolar planetary systems (e.g. Dvorak & Schwarz 2005; Schwarz et al. 2007). The present method is then quite relevant to the question of *habitability* of such planets, since the stability of *all* the proper elements (besides the semimajor axis) is an obvious prerequisite for habitability.

Our formalism contains the following steps.

(i) A precise 4D implicit symplectic mapping is derived, representing the co-orbital motion in the planar ERTBP, along the lines suggested by Sándor & Érdi (2003). In this, the disturbing function is expanded to terms of sufficient degree in the eccentricities of the disturbing body (Jupiter) and the test body (asteroid) and also in the variations of the semimajor axis of the test body.

(ii) The mapping is made explicit by series expansion and reversion around its main elliptic fixed point. This second step introduces a restriction of the domain of convergence of the explicit mapping. In the case of Jupiter's Trojans, the domain of convergence extends to free eccentricites $e_{\rm free} = 0.025$, i.e. below the upper limit of 'paradoxal' motions (Beaugé & Roig 2001), which in the ERTPB corresponds to a free eccentricity nearly equal to the forced one, i.e. $e_{\rm free} = e' \simeq 0.0487$. The small domain of convergence of the explicit mapping constitutes presently our main limitation as regards the investigation of Nekhoroshev stability in the case of Jupiter's Trojans. A different expansion in action-angle variables in the Laplace–Lagrange plane is under investigation.

(iii) An algorithm is constructed for the Birkhoff normalization of the explicit 4D mapping and the integrals of motion of the associated normal form are translated into proper element values.

(iv) The domain of Nekhoroshev stability is determined by the request that the remainder of the normal form cannot produce large variations of the integrals of motion up to a time exceeding the age of the Solar System. As expected in any pertubation theory, the so-determined domain is smaller than the domain found by numerical integrations (e.g. Levison, Shoemaker & Shoemaker 1997; Tsiganis, Varvoglis & Dvorak 2005, for the Jupiter's Trojans). Furthermore, this model is still quite simple and cannot account for the resonant transport of asteroids towards the edge of the stability zone due to the effects of the outer Solar System planets (Robutel, Gabern & Jorba 2005). Nevertheless, the analytically determined domain with the present model provides a relevant estimate and includes some real asteroids.

Section 2 describes the basic model as well as the derivation of an explicit symplectic mapping model for the Trojan problem from the associated averaged Hamiltonian. Section 3 gives the algorithm of calculation of the Birkhoff normal form for the 4D symplectic mapping.

Section 4 contains the main results, i.e. calculation of the size of the remainder and derivation of the domain of Nekhoroshev stability for the Jupiter's Trojans. We furthermore analyse the propagation of small divisors in the series, and show their influence on the size of the remainder, which yields the effective stability region. Section 5 summarizes the main conclusions of the present study.

2 THE MAPPING MODEL

2.1 Hamiltonian

The Hamiltonian of the planar ERTBP in the 1:1 resonance can be expressed in terms of modified Delaunay-like variables (Brown & Shook 1964):

$$x = \sqrt{\frac{a}{a'}} - 1, \quad \tau = \lambda - \lambda',$$
$$y = \sqrt{\frac{a}{a'}}\left(\sqrt{1-e^2} - 1\right), \quad \omega, \tag{2}$$

where a is the semimajor axis, e is the eccentricity, λ is the mean longitude, ω is the longitude of perihelion of the massless body and the primed variables refer to the disturbing body. The Hamiltonian reads

$$H = H_0 + \mu H_1 = -\frac{1}{2(1+x)^2} - (1+x) - \mu R, \tag{3}$$

where $\mu = m'/(m_0 + m')$ is the mass ratio of the primaries (we assume $m_0 \gg m'$) and R is the disturbing function given by

$$R = a'\left(\frac{1}{\Delta} - \frac{1}{r} + \frac{1}{2}\frac{\Delta^2}{r'^3} - \frac{1}{2}\frac{r^2}{r'^3}\right), \tag{4}$$

where r and r' are the distances of the massless body and of the smaller primary from the position of m_0, respectively. The distance Δ of the massless body from the disturbing body is given in Euclidian coordinates by

$$\Delta = \sqrt{r^2 + r'^2 - 2rr'\cos(\phi)}, \tag{5}$$

where the angle ϕ is between the vectors of the radii r and r'. The variables (τ, x), (ω, y) are canonical pairs satisfying the Hamiltonian equations:

$$\dot{\tau} = \frac{\partial H}{\partial x}, \quad \dot{x} = -\frac{\partial H}{\partial \tau}, \quad \dot{\omega} = \frac{\partial H}{\partial y}, \quad \dot{y} = -\frac{\partial H}{\partial \omega}. \tag{6}$$

Using the well-known relations between the true (u) and the mean (M) anomalies involving Bessel functions (e.g. Stumpff 1965):

$$\cos(u) = \frac{2\left(1-e^2\right)}{e}\left[\sum_{\nu=1}^{\infty} J_\nu(\nu e)\cos(\nu M)\right] - e,$$
$$\sin(u) = 2\sqrt{1-e^2}\sum_{\nu=1}^{\infty}\frac{1}{2}\left[J_{\nu-1}(e\nu) - J_{\nu+1}(e\nu)\right]\sin(M\nu), \tag{7}$$

we can rewrite $\cos(\phi)$, knowing the fact that

$$\cos(\phi) = \cos(u - u' + \omega - \omega'), \tag{8}$$

as a multivariate series in the eccentricites of the smaller body e and of the disturbing planet e', namely

$$\cos(\phi) = \cos(M - M' + \omega - \omega') + [-e'\cos(M + \omega - \omega') + e'\cos(M - 2M' + \omega - \omega') + e\cos(2M - M' + \omega - \omega')$$
$$- e\cos(M' - \omega + \omega')] + \cdots. \tag{9}$$

The distances r and r' are expressed in terms of the mean anomalies M, M', the eccentricities e, e' and the semimajor axes a, a' via a formula

$$r = a\left[1 + \frac{e^2}{2} - 2\left\{\sum_{\nu=1}^{\infty}\frac{\left[J_{\nu-1}(e\nu) - J_{\nu+1}(e\nu)\right]\cos(M\nu)}{2\nu}\right\}e\right], \tag{10}$$

and similarly for the primed variables. In view of (9) and (10), the disturbing function is written as a function of the form $R(a, a', e, e', \omega, \omega', M, M')$. Without loss of generality, we may set the fixed perihelion of the disturbing body equal to $\omega' = 0$. Introducing mean longitudes via $M = \lambda - \omega$, $M' = \lambda'$ and the critical argument τ via $\lambda = \lambda' + \tau$, we then arrive at an expression for R as a function of a, a', e, e', ω, τ and λ'. All the primed variables in this expression have fixed values except for λ' which increases linearly in time according to the mean motion of the disturbing planet. Developing further up to terms of fourth order in the eccentricities e or e' results in a series of the form

$$R(a, a', e, e', \omega, \tau, \lambda') = \sum_{\nu=1}^{\nu_{\max}} A_\nu(a, a', e, e', \tau)\cos\left[\varphi_\nu(\tau, \omega, \lambda')\right], \tag{11}$$

where the amplitude terms A_ν are polynomial in e, e', the angles φ_ν are linear combinations of their arguments and $\nu_{\max}$ is equal to the number of all possible trigonometric combinations of the angles consistent with d'Alembert's rule up to a given order of expansion in the

eccentricities. The terms A_ν are either of the form

$$A_\nu = \frac{\alpha_\nu(a, a', e, e')}{N_\nu \left(a^2 + a'^2 - 2aa' \cos\tau\right)^{p_\nu/2}} \tag{12}$$

or

$$A_\nu = \frac{\alpha_\nu(e, e')}{\gamma_\nu(a, a')}, \tag{13}$$

where α_ν, γ_ν are again polynomial in e, e', and N_ν, p_ν are integer numbers. In the former case, we can consider $\cos\tau$ as a small quantity as far as $|\tau|$ is not very close to zero (meaning close encounter of the massless body with the disturbing one). If this condition is satisfied (e.g. in our case for the Jupiter's Trojans), we can develop the terms (12) in powers of $\cos(\tau)$, then replace a by x and e by y, yielding thus the final form of the disturbing function as

$$R(\tau, \omega, x, y; a', e') = \sum_{\nu=1}^{\nu_{\max}} B_\nu(x, y, ; a', e') \cos\left[\Phi_\nu(\tau, \omega, \lambda')\right], \tag{14}$$

with new coefficients B_ν depending on A_ν and on the coefficients of the trigonometric expansions, and new angles $\Phi_\nu(\tau, \omega, \lambda')$ depending again linearly on their arguments. In our case of Jupiter's Trojans, we set the parameters equal to $\mu = 0.000\,954\,7919, \ldots, a' = 1$ and $e' = 0.0487\ldots$

2.2 Implicit mapping model

Let $H(J, J_\mathrm{f}, \theta, \theta_\mathrm{f})$ be a D d.o.f. Hamiltonian system in action-angle variables, J, θ denoting $D-1$ dimensional vectors and $J_\mathrm{f}, \theta_\mathrm{f}$ denoting a conjugate pair such that θ_f is a fast angle with period T significantly shorter than the periods associated with the remaining pairs. According to Hadjidemetriou's method (Hadjidemetriou 1991), a mapping approximating the Poincaré section of the Hamiltonian can be constructed by averaging H with respect to the fast angle and inserting the averaged Hamiltonian $\bar{H}$ in the generating function

$$W = J_{n+1} \cdot \theta_n + T\bar{H}(J_{n+1}, \theta_n). \tag{15}$$

The mapping is given by

$$J_{i,n} = \frac{\partial W}{\partial \theta_{i,n}}, \quad \theta_{i,n+1} = \frac{\partial W}{\partial J_{i,n+1}}, \quad i = 1, \ldots, D-1, \tag{16}$$

where $J_{i,n}$, $\theta_{i,n}$ and $J_{i,n+1}$, $\theta_{i,n+1}$ are the components of the vectors (J, θ) at the nth and $(n+1)$th mapping iterations, respectively. In applying (16), it is checked that the periodic orbits of the original system correspond to fixed points of the symplectic mapping which have the same stability.

In the case of the Hamiltonian (3), the fast angle is λ' and the remaining action-angle pairs are (x, τ) and (y, ω). An averaged Hamiltonian is then obtained via

$$\bar{H} = H_0 + \mu\bar{R} = H_0 + \mu\bar{R}(\tau, \omega, x, y; a', e') = H_0 + \mu\frac{1}{2\pi}\int_0^{2\pi} R(\tau, \omega, x, y; a', e', \lambda')\,\mathrm{d}\lambda'. \tag{17}$$

In the circular problem ($e' = 0$), it can be readily shown that in all the trigonometric arguments of (14) the angle λ' appears only via a combination $\lambda' - \omega$. Thus, through the averaging (17), the angle ω disappears as well from $\bar{H}$, and hence from the generating function (15). This implies that y becomes an integral of the mapping corresponding to the proper eccentricity, which simply becomes a label of a 2D symplectic mapping in the variables (x, τ). On the other hand, when e' is switched on there are terms depending on ω which survive the averaging (17). Thus, the new mapping is 4D and the dynamics of the action y is coupled to the dynamics of the pair (τ, x). In particular, the generating function takes the form

$$W = \tau_n x_{n+1} + \omega_n y_{n+1} - T\left[\frac{1}{2(1+x_{n+1})^2} + (1 + x_{n+1}) + \mu\bar{R}(\tau_n, \omega_n, x_{n+1}, y_{n+1}; a', e')\right] \tag{18}$$

and the mapping for the massless body is found via (16) [where the angles and actions are (τ, ω) and (x, y), respectively]. We set $T = 2\pi$, which corresponds to units of time in which the mean motion of the disturbing planet is equal to unity. The mapping is implicit, i.e. of the form

$$\begin{aligned}
\tau_{n+1} &= \tau_n + f_\tau(\tau_n, \omega_n, x_n, y_n, x_{n+1}, y_{n+1}), \quad x_n = x_{n+1} + f_x(\tau_n, \omega_n, x_n, y_n, x_{n+1}, y_{n+1}), \\
\omega_{n+1} &= \omega_n + f_\omega(\tau_n, \omega_n, x_n, y_n, x_{n+1}, y_{n+1}), \quad y_n = y_{n+1} + f_y(\tau_n, \omega_n, x_n, y_n, x_{n+1}, y_{n+1}).
\end{aligned} \tag{19}$$

The mapping (19) possesses the elliptic fixed points (Sándor & Érdi 2003)

$$(\tau_*, \omega_*, x_*, y_*) = \left(\pm\pi/3, \pm\pi/3, 0, \sqrt{1 - e'^2} - 1\right) \tag{20}$$

corresponding to two stable short-period orbits around L_4 and L_5, respectively. The 2D projections on the (τ, x) and (ω, y) planes for the case of Jupiter's Trojans (Figs 1a and b) of the 4D Poincaré surface of section yield the familiar picture of the dynamics of the co-orbital motion in the ERTBP. Figs 1(c) and (d) show the same projections obtained in a numerical integration of the exact Hamiltonian model. These compare well with the corresponding portraits by Hadjidemetriou's mapping: the angular tilt of the invariant curves in Fig. 1(a) with respect

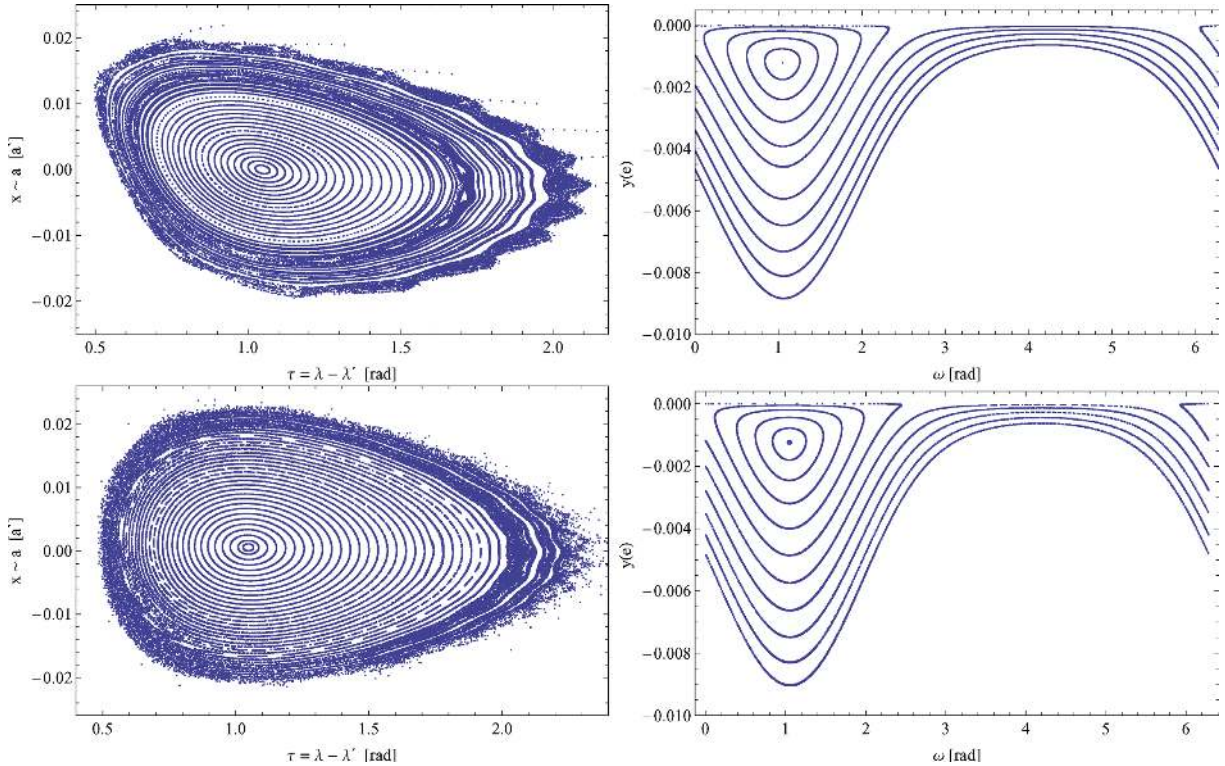

Figure 1. Phase portraits for the Trojan case of Jupiter in the Hadjidemetriou's mapping approach (upper line, 1a, 1b) versus the 4D Poincaré section of the exact Hamiltonian flow (lower line, 1c, 1d). The figures show sections of the 4D Poincaré surface of section manifold, namely: left-hand side column: section defined by $\omega_n = \omega_0$, $\omega_{n+1} - \omega_n > 0$, projected to the (τ, x) plane. Right-hand side column: section defined by $\tau_n = \tau_0$, $\tau_{n+1} - \tau_n > 0$ and $x_n > 0$ projected to the (ω, y) plane.

to Fig. 1(c) corresponds to a small phase difference $\Delta\theta$ in the oscillations of τ and x which is introduced by Hadjidemetriou's mapping (see section 2 of Efthymiopoulos & Sándor 2005). The visual impression of the tilt is only due to the very different scale of the axes in Figs 1(a) and (c). The value of $\Delta\theta$ is of the order of 10^{-2} rad. Furthermore, Fig. 1(c) shows a small chaotic zone at libration amplitudes $D \approx 25^0$, which, however, is well beyond the estimated area of Nekhoroshev stability (Section 4 below).

The regular motions on the (τ, x) plane are librational, and the border of the stability region is marked by high-order resonances creating island chains embedded in a chaotic stickiness zone. The relation between the libration amplitudes $D_{\rm p} = \tau_{\rm max} - \tau_{\rm min}$ and $d_{\rm p} = a_{\rm max} - a_{\rm min}$ calculated for different invariant curves of Fig. 1(a) is shown in Fig. 2(b). This relation is almost perfectly linear, and the slope is found to be 1/0.275 (in units rad/au), which almost coincides with the theoretical value given by Érdi (1988), not based on a mapping model. On the other hand, the regular motions appear in the plane (ω, y) either as librational [i.e. the perihelion of the asteroid librates between two values $0 < \omega_{\rm min} \leq \omega \leq \omega_{\rm max} < 2\pi$], or rotational ($0 \leq \omega \leq 2\pi$). The former motions correspond to the ERTBP limit of the motions called by Beaugé and Roig 'paradoxal', while the latter motions correspond to the 'non-paradoxal' motions. This terminology emphasizes that the difference of the two types of motion on the plane (ω, y) does not correspond to a seperatrix resonant dynamics. A plot in a Laplace–Lagrange section (Fig. 2a) shows that all the invariant curves are actually librational around a fixed centre. In the limit of the ERTBP, the centre is given by $[e' \cos(\pi/3), e' \sin(\pi/3)]$ and the radius of a librational curve $e_{\rm free}$ coincides with the proper eccentricity $e_{\rm p}$, i.e. it is an approximate integral of motion that characterizes, together with the other proper elements $D_{\rm p}$, $d_{\rm p}$, the motion on a particular invariant torus of the 4D mapping (19).

2.3 Explicit mapping model and diagonalization

The next step in the analytical procedure is to render the mapping (19) explicit, diagonalize and expand around one of the fixed points (20). Doing so involves the following substeps.

(i) *Development of the generating function* (18). We developed up to 16th order in the action-angle variables around the fixed point (20) and checked that the 16th order yields numerical values of W which are accurate within machine precision. It has to be stressed that it is preferable to develop the generating function W, and then re-derive the mapping, instead of Taylor expanding the mapping (19) itself, since any elaboration of the generating function does not affect the symplecticity of the mapping derived by it. Furthermore, it can be readily shown that if the centre of expansion of W is a fixed point of its mapping, then, after the expansion of W, the resulting mapping has a fixed point at the origin which has the same stability as the old fixed point.

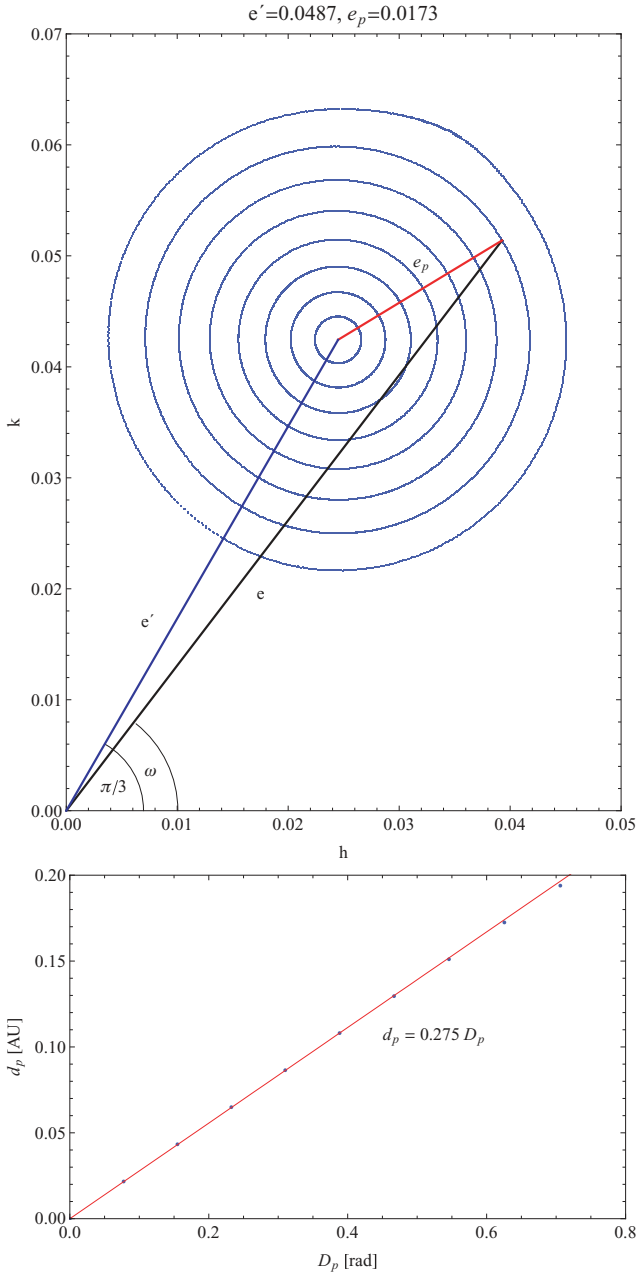

Figure 2. Analysis of the iteration data of the mapping model, for the case of Jupiter: Laplace–Lagrange plane [$h = e \cdot \cos(\omega)$, $k = e \cdot \cos(\omega)$] (2a) calculated from the mapping data which shows the librational behaviour around its fixed centre. The radius of the free eccentricities corresponds to the proper eccentricity given in Fig. 3. The lower figure (2b) shows the relationship between the proper elements $d_{\rm p}$ and $D_{\rm p}$ (see the text for definition), calculated from the mappping model in Fig. 1(a) for different invariant curves.

(ii) *Mapping reversal*. The mapping resulting from (i) reads

$$\begin{pmatrix} u_{1,n+1} \\ u_{2,n+1} \\ v_{1,n} \\ v_{2,n} \end{pmatrix} = \begin{pmatrix} u_{1,n} + U_{1,\text{linear}}(u_{1,n}, u_{2,n}, v_{1,n+1}, v_{2,n+1}) + U_{1,\text{non-linear}}(u_{1,n}, u_{2,n}, v_{1,n+1}, v_{2,n+1}) \\ u_{2,n} + U_{2,\text{linear}}(u_{1,n}, u_{2,n}, v_{1,n+1}, v_{2,n+1}) + U_{2,\text{non-linear}}(u_{1,n}, u_{2,n}, v_{1,n+1}, v_{2,n+1}) \\ v_{1,n+1} + V_{1,\text{linear}}(u_{1,n}, u_{2,n}, v_{1,n+1}, v_{2,n+1}) + V_{1,\text{non-linear}}(u_{1,n}, u_{2,n}, v_{1,n+1}, v_{2,n+1}) \\ v_{2,n+1} + V_{2,\text{linear}}(u_{1,n}, u_{2,n}, v_{1,n+1}, v_{2,n+1}) + V_{2,\text{non-linear}}(u_{1,n}, u_{2,n}, v_{1,n+1}, v_{2,n+1}) \end{pmatrix} \tag{21}$$

where the new variables $u_1 \equiv \tau - \tau_*$, $u_2 \equiv \omega - \omega_*$, $v_1 \equiv x - x_*$, $v_2 \equiv y - y_*$ are introduced and the functions U, V are polynomial, consisting of monomials of the form $C_{\{v_i\}} u_{1,n}^{v_1} u_{2,n}^{v_2} v_{1,n}^{v_3} v_{2,n}^{v_4} v_{1,n+1}^{v_5} v_{2,n+1}^{v_6}$ with real coefficients $C_{\{v_i\}}$ and terms satisfying the truncation condition of the generating function, that is, $\sum_i v_i \leq 16$. To find the mapping in its explicit form, we solve the system with respect to the linear part in ($v_{1,n+1}$, $v_{2,n+1}$) and use iterative series reversion until all monomials containing terms with $v_{1,n+1}$ or $v_{2,n+1}$ are pushed to orders higher than some order M. Actually in doing this reversal symplecticity is lost after the order M. However, if M is high enough the error in the preservation of Poisson

brackets can be suppressed to the machine precision. We pushed the reversion up to $M = 19$, resulting in approximately 10^5 coefficients of the multivariate polynomials. We used sparse array representation and pattern matching (storing multiple occurrences of coefficients just once) in order to reduce the memory space needed to store the large amount of coefficients and exponents. The error in the preservation of the Poisson structure turned out to be 10^{-10} at this order. This error affects the relative size of all mapping quantities (normal form, remainder) by an error of the same order beyond the normalization order $M = 19$.

(iii) *Diagonalization and complexification*. The Birkhoff normalization algorithm works more easily in complex canonical variables in which the linear part of the mapping is diagonal. In the case of Jupiter's Trojans, the linear part of the mapping (21) reads after reversion:

$$\begin{pmatrix} u_{1,n+1} \\ u_{2,n+1} \\ v_{1,n+1} \\ v_{2,n+1} \end{pmatrix} = \boldsymbol{M} \cdot \begin{pmatrix} u_{1,n} \\ u_{2,n} \\ v_{1,n} \\ v_{2,n} \end{pmatrix} = \begin{pmatrix} 724.471 \times 10^{-3} & 1.592\,77 \times 10^{-3} & -19.0939 & -10.1437 \times 10^{-3} \\ 552.164 \times 10^{-6} & 999.587 \times 10^{-3} & -9.982\,92 \times 10^{-3} & -8.4445 \\ 13.8281 \times 10^{-3} & -82.7724 \times 10^{-6} & 1.015\,87 & 0 \\ -81.9979 \times 10^{-6} & 48.9957 \times 10^{-6} & -38.1077 \times 10^{-6} & 1. \end{pmatrix} \cdot \begin{pmatrix} u_{1,n} \\ u_{2,n} \\ v_{1,n} \\ v_{2,n} \end{pmatrix} \tag{22}$$

The transformation from the set of real (u_1, u_2, v_1, v_2) to the set of complex conjugate canonical variables $(z_1, z_2, \overline{z_1}, \overline{z_2})$ comes from a standard procedure, namely (i) calculating the eigenvectors of $\boldsymbol{M}^T$ and (ii) rescaling the linear transformation induced by the matrix of eigenvectors so as to preserve the Poisson structure $\{z_i, \overline{z_j}\} = i\delta_{ij}$, $\{z_i, z_j\} = \{\overline{z_i}, \overline{z_j}\} = 0$. The final transformation in our case reads

$$\boldsymbol{z} = \boldsymbol{B} \cdot \boldsymbol{u}, \tag{23}$$

where $\boldsymbol{z} \equiv (z_1, z_2, \overline{z_1}, \overline{z_2})^T$, $\boldsymbol{u} \equiv (u_1, u_2, v_1, v_2)^T$ and

$$\boldsymbol{B} = \begin{pmatrix} 33.5883 \times 10^{-3} & -188.273 \times 10^{-6} & 4.401\,64 & -9.354\,07 \times 10^{-3} \\ 43.8972 \times 10^{-6} & 350.249 \times 10^{-6} & 86.6193 \times 10^{-3} & 14.4442 \\ 33.5883 \times 10^{-3} & -188.273 \times 10^{-6} & 4.401\,64 & -9.354\,07 \times 10^{-3} \\ 43.8972 \times 10^{-6} & 350.249 \times 10^{-6} & 86.6193 \times 10^{-3} & 14.4442 \end{pmatrix}$$
$$+ i \begin{pmatrix} -113.593 \times 10^{-3} & 681.194 \times 10^{-6} & 0 & -70.4576 \times 10^{-6} \\ -73.7266 \times 10^{-6} & -34.6156 \times 10^{-3} & -21.4709 \times 10^{-6} & 0 \\ 113.593 \times 10^{-3} & -681.194 \times 10^{-6} & 0 & 70.4576 \times 10^{-6} \\ 73.7266 \times 10^{-6} & 34.6156 \times 10^{-3} & 21.4709 \times 10^{-6} & 0 \end{pmatrix}.$$

In the complex canonical variables, the linearized mapping then reads

$$z_1' = \mathrm{e}^{\frac{2\pi \mathrm{i}}{T_1}} z_1, \qquad z_2' = \mathrm{e}^{\frac{2\pi \mathrm{i}}{T_2}} z_2, \tag{24}$$

where the basic periods are derived from the eigenvalues $(\Lambda_1, \overline{\Lambda}_1, \Lambda_2, \overline{\Lambda}_2)$ of the matrix $\boldsymbol{M}$ via $T_j = 1/\cos^{-1}[\mathrm{Re}\,(\Lambda_j)]$, $j = 1, 2$; and in our case, they are equal to $T_1 = 12.1944$ and $T_2 = 310.453$. In these expressions, the periods are given in units of Jupiter's period, which, in the present time units, is $T_{\mathrm{Jup}} = 2\pi$. Translated to years the periods turn out to be

$$T_1 \to T_{\mathrm{short}} = 144.626\,\mathrm{yrs}, \quad T_2 \to T_{\mathrm{long}} = 3681.97\,\mathrm{yrs}. \tag{25}$$

These values, derived by the mapping approach, differ by less than 3 per cent from the values given in Érdi (1997), namely $T_1 = 3683.97$ and $T_2 = 147.8$ yr.

3 BIRKHOFF NORMALIZATION AND NEKHOROSHEV STABILITY ESTIMATES

3.1 Birkhoff normal form

Having determined the explicit mapping in the vicinity of L_4 or L_5, we proceed now in implementing the main analytical apparatus of the Nekhoroshev theory, namely the calculation of a Birkhoff normal form of which the remainder (at the optimal size of truncation) yields the estimates of Nekhoroshev stability. Precisely, let

$$\begin{aligned} z_1' &= F_1(z_1, z_2, \bar{z}_1, \bar{z}_2), \\ z_2' &= F_2(z_1, z_2, \bar{z}_1, \bar{z}_2), \end{aligned} \tag{26}$$

be a 4D symplectic mapping in complex canonical variables with functions F_i, $i = 1, 2$ of the form:

$$F_i = \Omega_{\omega,i} z_i + \sum_{n \geq 2}^{M} F_{i,n}(z_1, z_2, \bar{z}_1, \bar{z}_2)\,, \tag{27}$$

where $\boldsymbol{\Omega_\omega} = (\mathrm{e}^{\mathrm{i}\omega_1}, \mathrm{e}^{\mathrm{i}\omega_2})$ is a vector of complex numbers associated with the linear frequency vector of the unperturbed twist mapping $\boldsymbol{\omega} = (\omega_1, \omega_2)$, and the functions $F_{i,n}$ $(i = 1, 2)$ are complex polynomial functions of the order of n, holding together monomials of the form $D_{a,b,c,d} \cdot z_1^a \bar{z}_1^b z_2^c \bar{z}_2^d$ with $a + b + c + d = n$. We assume that the frequencies (ω_1, ω_2) are incommensurable. The purpose of the Birkhoff normalization is to introduce a canonical transformation $\boldsymbol{z} = \boldsymbol{\Phi}(\boldsymbol{\zeta})$ via transformation functions $\boldsymbol{\Phi} \equiv (\Phi_1, \Phi_2, \bar{\Phi}_1, \bar{\Phi}_2)$ such that in the new

variables $\boldsymbol{\zeta}$ the mapping resumes a particularly simple form unraveling the existence of approximate integrals of motion, namely

$$\boldsymbol{\zeta}' = \boldsymbol{U}(\boldsymbol{\zeta}) + \boldsymbol{R}(\boldsymbol{\zeta}), \tag{28}$$

where the set of functions $\boldsymbol{U} \equiv (U_1, U_2, \bar{U}_1, \bar{U}_2), i = 1, 2$ represents an integrable mapping and $\boldsymbol{R}$ is the vector of remainder functions representing a small perturbation to the integrable mapping. In the non-resonant case, the mapping $\boldsymbol{U}$ is a twist mapping. The main result of Nekhoroshev theory is that by an appropriate transformation $\boldsymbol{\Phi}$, the size of $\boldsymbol{R}$ can be rendered exponentially small in a properly defined small parameter. This guarantees an exponentially long practical stability, i.e. preservation of the integrals of the normal form mapping $\boldsymbol{U}$, for the orbits under the full mapping (28). In doing the normalization, we implement the 4D analog of the algorithm of Servizi et al. (1983), see also Bazzani, Marmi & Turchetti (1990). Writing the unknown functions $\boldsymbol{\Phi}$ and $\boldsymbol{U}$ as

$$\Phi_i = \Phi_i(\boldsymbol{\zeta}) = \zeta_i + \sum_{n\geq 2}^{M} \Phi_{i,n}\left(\zeta_1, \zeta_2, \bar{\zeta}_1, \bar{\zeta}_2\right) \tag{29}$$

and

$$U_i = U_i(\boldsymbol{\zeta}) = \Omega_{\omega,i}\zeta_i + \sum_{n\geq 2}^{M} U_{i,n}\left(\zeta_1, \zeta_2, \bar{\zeta}_1, \bar{\zeta}_2\right), \tag{30}$$

where the functions $\Phi_{i,n}$ and $U_{i,n}$, $(i = 1, 2)$ are of the same polynomial form as the functions $F_{i,n}$, the unknown functions are determined step by step by splitting the homological equation

$$\boldsymbol{\Phi} \circ \boldsymbol{U} = \boldsymbol{F} \circ \boldsymbol{\Phi} \tag{31}$$

into terms of the same order (the symbol $\circ$ denotes polynomial composition). Defining the projection operators

$$[f]_N = f_N, \tag{32}$$

$$[f]_{<N} = \sum_{k<N} f_k = f_0 + f_1 + \ldots + f_{N-1} \tag{33}$$

and

$$[f]_{\leq N} = \sum_{k\leq N} f_k = f_0 + f_1 + \ldots + f_N \tag{34}$$

which act on either scalar or vector functions f, the Nth order terms of the homological equation yield

$$\boldsymbol{\Delta}_{\boldsymbol{\omega}}[\boldsymbol{\Phi}(\boldsymbol{\zeta})]_N + [\boldsymbol{U}(\boldsymbol{\zeta})]_N = [[\boldsymbol{F}]_{\leq N}\{[\boldsymbol{\Phi}(\boldsymbol{\zeta})]_{<N}\}]_N - [\boldsymbol{\Phi}]_{<N}([\boldsymbol{U}(\boldsymbol{\zeta})]_{<N})_N \equiv [\boldsymbol{R}]_N, \tag{35}$$

where we have defined the linear operator: $\boldsymbol{\Delta}_{\boldsymbol{\omega}} = (\Delta_{\omega,1},\ \Delta_{\omega,2},\ \bar{\Delta}_{\omega,1},\ \bar{\Delta}_{\omega,2})$ according to $\boldsymbol{\Delta}_{\boldsymbol{\omega}}[\boldsymbol{\Phi}(\boldsymbol{\zeta})]_N \equiv [\boldsymbol{\Phi}(\boldsymbol{\Omega}_\omega \cdot \boldsymbol{\zeta})]_N - \boldsymbol{\Omega}_\omega \cdot [\boldsymbol{\Phi}(\boldsymbol{\zeta})]_N$, or, in component notation:

$$\begin{aligned}
\Delta_{\omega,1}\,[\Phi_1(\boldsymbol{\zeta})]_N &= \left[\Phi_1\left(\Omega_{\omega,1}\cdot\boldsymbol{\zeta}\right)\right]_N - \Omega_{\omega,1}\cdot[\,\Phi_1(\boldsymbol{\zeta})]_N\,,\\
\Delta_{\omega,2}\,[\Phi_2(\boldsymbol{\zeta})]_N &= \left[\Phi_2\left(\Omega_{\omega,2}\cdot\boldsymbol{\zeta}\right)\right]_N - \Omega_{\omega,2}\cdot[\,\Phi_2(\boldsymbol{\zeta})]_N\,.
\end{aligned} \tag{36}$$

Equation (35) can be solved recursively to specify the unknown functions $[\boldsymbol{U}]_N$ and $[\boldsymbol{\Phi}]_N$ starting with $[\boldsymbol{U}]_1 = [\boldsymbol{F}]_1$ and $[\boldsymbol{\Phi}]_1 = \boldsymbol{\zeta}$. The solution at the Nth step is found by noting that all the quantities appearing in the right-hand side of (35) are already specified in the previous steps, that is, $[\boldsymbol{R}]_N$ is a known function. Furthermore, all monomials of the form $\zeta_1^{\alpha_1}\bar{\zeta}_1^{\beta_1}\zeta_2^{\alpha_2}\bar{\zeta}_2^{\beta_2}$ are eigenfunctions of the operators Δ_{ω_i} with eigenvalues $\mathrm{e}^{\mathrm{i}(\alpha_1-\alpha_2)\omega_1+i(\beta_1-\beta_2)\omega_2} - \mathrm{e}^{\mathrm{i}\omega_i},\ i = 1, 2$, respectively. In the non-resonant case, the kernels of these operators are defined as $(k, l = 1, 2, \ldots)$

$$\begin{aligned}
&\ker(\Delta_{\omega_1}) = \{\text{monomials of the form } \zeta_1^{k+1}\bar{\zeta}_1^{k}\zeta_2^{l}\bar{\zeta}_2^{l}\}\\
&\ker(\Delta_{\omega_2}) = \{\text{monomials of the form } \zeta_1^{k}\bar{\zeta}_1^{k}\zeta_2^{l+1}\bar{\zeta}_2^{l}\}.
\end{aligned} \tag{37}$$

The definition of the kernels via (37) allows one to solve (35) for both the unknown functions $[\boldsymbol{U}]_N$ and $[\boldsymbol{\Phi}]_N$. The solution is

$$\begin{aligned}
&[U_i]_N = \text{terms of } ker(\Delta_{\omega_i}) \text{ in } [R_i]_N,\\
&[\Phi_i]_N = \Delta_{\omega_i}^{-1}([Q_i]_N) \equiv \{\text{terms of } \mathcal{R}(\Delta_{\omega_i}) \text{ in } [R_i]_N\},\quad i = 1, 2,
\end{aligned} \tag{38}$$

where $\mathcal{R}(\Delta_{\omega_i})$ denotes the range of the respective operator and the action of inverse operators is defined by

$$\Delta_{\omega_i}^{-1}\left(a_{\alpha_1,\alpha_2,\beta_1,\beta_2}\zeta_1^{\alpha_1}\bar{\zeta}_1^{\beta_1}\zeta_2^{\alpha_2}\bar{\zeta}_2^{\beta_2}\right) = a_{\alpha_1,\alpha_2,\beta_1,\beta_2}\frac{\zeta_1^{\alpha_1}\bar{\zeta}_1^{\beta_1}\zeta_2^{\alpha_2}\bar{\zeta}_2^{\beta_2}}{\mathrm{e}^{\mathrm{i}(\alpha_1-\alpha_2)\omega_1+\mathrm{i}(\beta_1-\beta_2)\omega_2} - \Omega_{\omega_i}}, i = 1, 2. \tag{39}$$

Knowing the form of normal form terms (37), we can conclude that there can only be normal form terms for odd orders and $U_{i,n} = \bar{U}_{i,n} = 0$ for n even. On the other hand, the form of the homological equations (35) implies that the equations are still satisfied by the addition of any kernel terms of the form (37) to the transformation functions Φ_{i} specified through the second of equations (38). We exploit this freedom in order to ensure that the transformation remains symplectic up to the order of N, by adding kernel terms at every odd order to the functions

(Φ_i) specified via (38), namely

$$[\Phi_1]_N \to [\Phi_1]_N + \sum_{k,l\geq 0,\ 2(k+l)+1=N} c_{1,k+1,l}\zeta_1^{k+1}\bar{\zeta}_1^{k}\zeta_2^{l}\bar{\zeta}_2^{l},$$

$$[\Phi_2]_N \to [\Phi_2]_N + \sum_{k,l\geq 0,\ 2(k+l)+1=N} c_{2,k,l+1}\zeta_1^{k}\bar{\zeta}_1^{k}\zeta_2^{l+1}\bar{\zeta}_2^{l}, \tag{40}$$

where the coefficients $c_{1,k+1,l}$ and $c_{2,k,l+1}$ are specified by the request that Poisson brackets be preserved up to terms of the order of $N-1$, namely

$$\begin{aligned}
P_1 &\equiv \left\{[\Phi_1]_N\,,\left[\bar{\Phi}_1\right]_N\right\} = 1 + O(N-1),\\
P_2 &\equiv \left\{[\Phi_2]_N\,,\left[\bar{\Phi}_2\right]_N\right\} = 1 + O(N-1),\\
P_3 &\equiv \{[\Phi_1]_N\,,[\Phi_2]_N\} = 0 + O(N-1).
\end{aligned} \tag{41}$$

This set of equations (41) yields the values of the coefficients (κ, k, $l = 1, 2\ldots$):

$$\begin{aligned}
\mathrm{Re}\left(c_{1,k+1,l}\right) &= -\mathrm{Re}\left[\mathrm{coeff}\left(P_1, \zeta_1^{k}\bar{\zeta}_1^{k}\zeta_2^{l}\bar{\zeta}_2^{l}\right)\right]/\,2\kappa,\\
\mathrm{Re}\left(c_{2,k,l+1}\right) &= -\mathrm{Re}\left[\mathrm{coeff}\left(P_2, \zeta_1^{k}\bar{\zeta}_1^{k}\zeta_2^{l}\bar{\zeta}_2^{l}\right)\right]/\,2\kappa,\\
\mathrm{Im}\left(c_{1,k+1,l}\right) &= \mathrm{Im}\left[\mathrm{coeff}\left(P_3, \zeta_1^{k+1}\bar{\zeta}_1^{k}\zeta_2^{l}\bar{\zeta}_2^{l-1}\right)\right]/\,l,\\
\mathrm{Im}\left(c_{2,k,l+1}\right) &= 0.
\end{aligned} \tag{42}$$

The above symplectification of the transformation functions completes one step of the normalization procedure. The speed of the algorithm mainly depends on the speed of the multivariate polynomial compositions involved in the right-hand side of (35). The authors implemented the algorithm in a combined MATHEMATICA/C++ program. Automated derivation methods (Lhotka 2004; Hagel & Lhotka 2005) based on numerical and symbolic language paradigma were combined to improve the performance and readability of the code: the implementation includes sparse representation of multivariate polynomials and a composition algorithm based on multivariate Horner form (so that the number of multiplications and additions of polynomials is minimized). The performance of the multivariate multiplications was optimized by calculating all convolutions via fast Fourier transform (FFT) methods. In addition, the program was parallelized to a grid of 5 PCs. For our Trojan model, we carried out expansions up to 25th order.

3.2 Remainder and Nekhoroshev stability estimates

The normal form mapping $[\boldsymbol{U}]_{\leq N}$ in the new variables becomes a twist mapping:

$$\begin{aligned}
\zeta_1' &= [U_1]_{\leq N}\left(\zeta_1, \zeta_2, \bar{\zeta}_1, \bar{\zeta}_2\right) = \mathrm{e}^{\mathrm{i}\Gamma_1(\zeta_1,\zeta_2,\bar{\zeta}_1,\bar{\zeta}_2)}\zeta_1,\\
\zeta_2' &= [U_2]_{\leq N}\left(\zeta_1, \zeta_2, \bar{\zeta}_1, \bar{\zeta}_2\right) = \mathrm{e}^{\mathrm{i}\Gamma_2(\zeta_1,\zeta_2,\bar{\zeta}_1,\bar{\zeta}_2)}\zeta_2,
\end{aligned} \tag{43}$$

where Γ_1 and Γ_2 depend only on products of equal powers of the new variables $\zeta_1\bar{\zeta}_1$ and $\zeta_2\bar{\zeta}_2$. The mapping (43) is integrable, the exact integrals being given by $I_1 = \zeta_1\bar{\zeta}_1,\ I_2 = \zeta_2\bar{\zeta}_2$. These integrals can be expressed in terms of the old variables in an open domain around the origin in which the transformations $[\Phi_i]_{\leq N}$ are invertible:

$$I_1 = (\Phi_1)^{-1}_{\leq N}(z_1, z_2, \bar{z}_1, \bar{z}_2)\cdot(\bar{\Phi}_1)^{-1}_{\leq N}(z_1, z_2, \bar{z}_1, \bar{z}_2)\,, \tag{44}$$

$$I_2 = (\Phi_2)^{-1}_{\leq N}(z_1, z_2, \bar{z}_1, \bar{z}_2)\cdot(\bar{\Phi}_2)^{-1}_{\leq N}(z_1, z_2, \bar{z}_1, \bar{z}_2) \tag{45}$$

The level curves $I_k = constant$ $(k = 1, 2)$ define two independent invariant circles in coordinates $(\zeta_1, \zeta_2, \bar{\zeta}_1, \bar{\zeta}_2)$ or $(z_1, z_2,\ \bar{z}_1,\ \bar{z}_2)$, respectively. An orbit defined for a pair of label values (I_1, I_2) lies on an invariant 2D torus of the phase space of the normal form mapping. If, however, the remainder terms of (28) are taken into account, the motion is possibly no longer integrable and a small drift of the orbits across the invariant tori of the normal form mapping is introduced. The Nekhoroshev estimates are obtained by providing upper bounds for the cumulative drift induced by the remainder terms of the mapping within a time equal to the age of the Solar System. The mapping in the new variables is given by

$$\begin{aligned}
\zeta_1' &= [\Phi_1]^{-1}_{\leq N}\circ F_1\circ\Phi_1 = [U_1]_{\leq N}\left(\zeta_1, \zeta_2, \bar{\zeta}_1, \bar{\zeta}_2\right) + R_1^{(N)}\left(\zeta_1, \zeta_2, \bar{\zeta}_1, \bar{\zeta}_2\right),\\
\zeta_2' &= [\Phi_2]^{-1}_{\leq N}\circ F_2\circ\Phi_2 = [U_2]_{\leq N}\left(\zeta_1, \zeta_2, \bar{\zeta}_1, \bar{\zeta}_2\right) + R_2^{(N)}\left(\zeta_1, \zeta_2, \bar{\zeta}_1, \bar{\zeta}_2\right).
\end{aligned} \tag{46}$$

The resulting mapping (46) is symplectic up to the order of N. The quantity $R^{(N)} = [R_1^{(N)}, R_2^{(N)}]$ is called the remainder at the Nth order of normalization. This is, in principle, an infinite series, which contains all the terms of orders beyond N produced by the terms of the original mapping defined by $\boldsymbol{F}$. The drift along tori is calculated by deriving, from (46), the so-called *mapping of radii* (or of the actions), given by multiplying each of the equations (46) by its complex conjugate ($\rho_1 = \zeta_1\bar{\zeta}_1$, $\rho_2 = \zeta_2\bar{\zeta}_2$):

$$\begin{aligned}
\rho_1'^2 &= \rho_1^2 + R_{1,\rho}^{(N)} = \rho_1^2 + \sum_{i+j=N+2}^{M} a_{i,j}^{(N)}\rho_1^i\rho_2^j = \rho_1^2 + \sum_{i+j=N+2}^{M} f_n^{(N)},\\
\rho_2'^2 &= \rho_2^2 + R_{2,\rho}^{(N)} = \rho_2^2 + \sum_{i+j=N+2}^{M} b_{i,j}^{(N)}\rho_1^i\rho_2^j = \rho_2^2 + \sum_{i+j=N+2}^{M} g_n^{(N)},
\end{aligned} \tag{47}$$

where the functions $f_n^{(N)}$, $g_n^{(N)}$ depend on all the four variables $\zeta_1 = \rho_1 e^{i\phi_1}$, $\bar{\zeta}_1 = \rho_1 e^{-i\phi_1}$, $\zeta_2 = \rho_2 e^{i\phi_2}$ and $\bar{\zeta}_2 = \rho_2 e^{-i\phi_2}$. In practice, we also truncate $\boldsymbol{R}^{(N)}$ at some high order M. The terms $R_1^{(N)}, R_2^{(N)}$ are called remainder terms of the mapping of radii. The domain of convergence of the mapping (47) is estimated by D'Alembert's criterion implemented to the majorant series of (47) in polar coordinates, the domain in the 2D space of radii ($\rho_1 \geq 0$, $\rho_2 \geq 0$). In order to cover the full domain, we consider a grid of direction angles $\gamma \in (0,\pi/2)$ defined by $\rho_1 = \rho_\gamma \cos(\gamma)$, $\rho_2 = \rho_\gamma \sin(\gamma)$ such that the majorant mapping of (47) reads

$$\rho_1'^2 = \rho_1^2 + \sum_{i+j=N+2}^{M} A_\gamma^{(n)} \cdot \rho_\gamma^n = \sum_{i+j=N+2}^{M} \left| f_n^{(N)} \right|^*, A_\gamma^{(n)} = \sum_{i+j=N+2}^{M} \left| a_{i,j}^{(N)} (\cos\gamma)^i (\sin\gamma)^j \right|, \tag{48}$$

$$\rho_2'^2 = \rho_2^2 + \sum_{i+j=N+2}^{M} B_\gamma^{(n)} \cdot \rho_\gamma^n = \sum_{i+j=N+2}^{M} \left| g_n^{(N)} \right|^*, B_\gamma^{(n)} = \sum_{i+j=N+2}^{M} \left| b_{i,j}^{(N)} (\cos\gamma)^i (\sin\gamma)^j \right|. \tag{49}$$

D'Alembert's rule for the convergence of the majorant mapping of radii now reads

$$\lim_{n\to\infty} \frac{\left| f_{n+1}^{(N)} \right|^*}{\left| f_n^{(N)} \right|^*} < q_1 < 1, \lim_{n\to\infty} \frac{\left| g_{n+1}^{(N)} \right|^*}{\left| g_n^{(N)} \right|^*} < q_2 < 1. \tag{50}$$

In order to determine the radius of convergence ρ_γ, we calculate numerically the ratios appearing in (50) up to a high order at which the ratios stabilize. For the original mapping ($N = 3$), we find numerically the stabilization after $n = 15$, and we extended the calculation up to $n = 25$ yielding the convergence radius as

$$\rho_\gamma < \min\left(\frac{1}{q_{1,\gamma}}, \frac{1}{q_{2,\gamma}}\right) = \min\left[\frac{A_\gamma^{(n)}}{A_\gamma^{(n+1)}}, \frac{B_\gamma^{(n)}}{B_\gamma^{(n+1)}}\right], \tag{51}$$

where $q_{i,\gamma}, i = 1, 2$ are defined through

$$\frac{A_\gamma^{(n+1)}}{A_\gamma^{(n)}} = q_{1,\gamma}, \quad \frac{B_\gamma^{(n+1)}}{B_\gamma^{(n)}} = q_{2,\gamma}, \quad n = 25. \tag{52}$$

In the next step, we estimate the size of the remainder and therefore determine the area of Nekhoroshev stability. Fixing again a particular direction γ in the plane of radii, the size of the remainder terms $R_{1,\rho}^{(N)}, R_{2,\rho}^{(N)}$ along this direction can be estimated by taking the majorant series of the remainder terms of the mapping of radii with the substitution $|\zeta_1| \equiv \rho_1 = \rho\cos\gamma$, $|\zeta_2| \equiv \rho_2 = \rho\sin\gamma$. Introducing the norm

$$\left\| R_{1,\rho}^{(N)} \right\|_\gamma = \sum_{\alpha+\beta\geq N+2} \left| c_{1,\alpha,\beta} \cdot \cos^\alpha\gamma \cdot \sin^\beta\gamma \right|,$$

$$\left\| R_{2,\rho}^{(N)} \right\|_\gamma = \sum_{\alpha+\beta\geq N+2} \left| c_{2,\alpha,\beta} \cdot \cos^\alpha\gamma \cdot \sin^\beta\gamma \right|, \tag{53}$$

the influence of the remainder terms after r iteration steps of the mapping is determined by giving an upper bound of how far away can the remainder terms cause an orbit to drift, when this orbit lies initially on a particular invariant torus of the normal form mapping labelled by two values (ρ_1, ρ_2), i.e. by a particular value of ρ (for fixed γ). Let ρ_f be an upper bound for the label of the final torus on which the orbit lies after the r-step drift. We then have $\rho_\mathrm{f}^2 - \rho^2 \leq r\|R_\rho^{(N)}\|\rho_\mathrm{f}^N$ or

$$r \geq \frac{\rho_\mathrm{f}^2 - \rho^2}{\left\| R_\rho^{(N)} \right\| \rho_\mathrm{f}^N} \equiv r_{\min}(\rho, \rho_\mathrm{f}). \tag{54}$$

The quantity $r_{\min}(\rho, \rho_\mathrm{f})$ yields a lower bound for the time (number of iterations) requested for an orbit to drift from the torus labelled by ρ to the torus labelled by ρ_f. We have $r_{\min}(\rho, \rho) = 0$, meaning that it takes no time for an orbit not to make any drift. However, we also have $\lim_{\rho_\mathrm{f}\to\infty} r_{\min}(\rho, \rho_\mathrm{f}) = 0$, meaning that if one estimates the size of the remainder through the whole drift, going from ρ to ρ_f, by its upper value at $\rho_\mathrm{f} \to \infty$, one finds an infinite size which implies that it is possible to accomplish the drift, again, at zero time. The optimal result is found by requesting that the final label ρ_f is as far as possible from ρ, and, at the same time, as small as possible so that the size of the remainder during the excursion from ρ to ρ_f is not seriously overestimated. Thus, the optimal value of ρ_f is given by rendering $r_{\min}(\rho, \rho_\mathrm{f})$ maximal, that is,

$$\frac{\mathrm{d}}{\mathrm{d}\rho_\mathrm{f}} \left(\frac{\rho_\mathrm{f}^2 - \rho^2}{\left\| R_\rho^{(N)} \right\| \rho_\mathrm{f}^N} \right) = 0,$$

yielding

$$\rho_\mathrm{f} = \rho\sqrt{\frac{N}{N-2}}. \tag{55}$$

Defining the Nekhoroshev time T_Nek to be the time after r iteration steps of the mapping, we get after inserting (55) into (54) for the relation $T_\mathrm{Nek}(\rho)$:

$$T_\mathrm{Nek} = \frac{\rho^2 \left(\frac{N}{N-2} - 1\right)}{\left\| R_\rho^{(N)} \right\| \rho^N \left(\frac{N}{N-2}\right)^N} = \frac{2}{(N-2)\left\| R_\rho^{(N)} \right\| \left(\frac{N}{N-2}\right)^N \rho^{N-2}} \tag{56}$$

which leads along the direction γ to the maximum distance $\rho\gamma$ from the equilibrium up to which an orbit can drift within a Nekhoroshev time $T_{\rm Nek}$, estimated by using the remainder R_ρ of the order of N:

$$\rho_\gamma = 2^{-\frac{1}{2-N}} \left[-(2-N) \left(\frac{N}{-2+N} \right)^N \left\| R_\rho^{(N)} \right\|_\gamma T_{\rm Nek} \right]^{\frac{1}{2-N}} . \tag{57}$$

Equation (57) serves as the basic result used in the sequel in order to construct our stability region.

4 APPLICATION TO JUPITER'S TROJANS

The domain of convergence of the original mapping of radii (47) on the (ρ_1, ρ_2) plane can be transformed to a domain of convergence in the space of proper elements $(D_{\rm p}, e_{\rm p})$. To this end, for a particular direction γ, we back transform the two-torus with radii $\rho_1 = \rho_\gamma \cos\gamma$ and $\rho_2 = \rho_\gamma \sin\gamma$ to complex variables using $z_1 = \rho_\gamma \cos\gamma e^{-i\varphi_1}$, $z_2 = \rho_\gamma \sin\gamma e^{-i\varphi_2}$, and scan the whole torus $(\varphi_1, \varphi_2) \in [0, 2\pi) \times [0, 2\pi)$ in order to find the maximum and the minimum values of the quantities $[\tau, \omega, x, h = e(y) \cos(\omega)]$. This torus is labelled by one pair of values of the proper elements $D_{\rm p}(\gamma) = (\tau_{\rm min} - \tau_{\rm max})/2$ and $e_{\rm p}(\gamma) = (h_{\rm min} - h_{\rm max})/2$. Plotting $D_{\rm p}(\gamma)$ versus $e_{\rm p}(\gamma), 0 \le \gamma \le \pi/2$ yields the boundary of the grey-shaded domain in Fig. 3, which corresponds to the domain of convergence of the mapping of radii (47) in the space of proper elements. On the other hand, for any particular direction γ in the space of radii $(\rho_1 = \rho_\gamma \cos\gamma, \rho_2 = \rho_\gamma \sin\gamma)$, the Nekhoroshev domain of stability is given by finding, through (57) with $T_{\rm Nek} = 10^9$, the value of the order of normalization N at which one obtains the optimal estimate, that is, the maximum value of ρ_γ. The dependencies of the order of normalization N, but also on the distance in phase space ρ along different directions γ are shown in Figs 4(a)–(c). The figures demonstrate the general asymptotic behavior expected for the Birkhoff series. Namely, the remainder initially decreases as N increases, giving the impression that it tends to zero as $N \to \infty$. However, this trend is reversed after an optimal order at which the remainder presents minimum, while beyond the optimal order the remainder increases as N increases, and its limiting size is infinite when $N \to \infty$, signifying the divergence of the Birkhoff normalization scheme. In Figs 4(a)–(c), we observe that for larger angles γ, i.e. higher proper eccentricities, the optimal normalization order is actually at orders exceeding our calculation limit $N = 25$, while for lower eccentricities the optimal order lies well beyond. This implies that our present calculations actually may underestimate along specific directions the true domain of Nekhoroshev stability. The boundary of the latter is shown as a solid line in Fig. 3, obtained by translating, for each value of γ, the radii ρ_1 and ρ_2 found from the optimal value of ρ_γ to proper element values. The dependency of the stability region on the direction, stemming from the dependency of the size of the remainder on the latter one, indicates that diffusion rates may dependent on it also, an insight which will be analysed in detail in upcoming projects.

The size of the remainder in (57), to determine the stability region, is determined by the more restrictive choice:

$$\left\| R_\rho^{(N)} \right\|_\gamma = \max \left[\left\| R_{1,\rho_2}^{(N)} \right\|_\gamma , \left\| R_{2,\rho_1}^{(N)} \right\|_\gamma \right] . \tag{58}$$

Additional remarks as regards Fig. 3 are the following.

(i) The original mapping of radii converges in a rather small zone of proper eccentricities ($e_{\rm p} < 0.025$). This constitutes presently our main limitation, because the upper limit of this domain is actually smaller than the upper limit of librational motions ($e_{\rm p} < 0.0487$). This limit

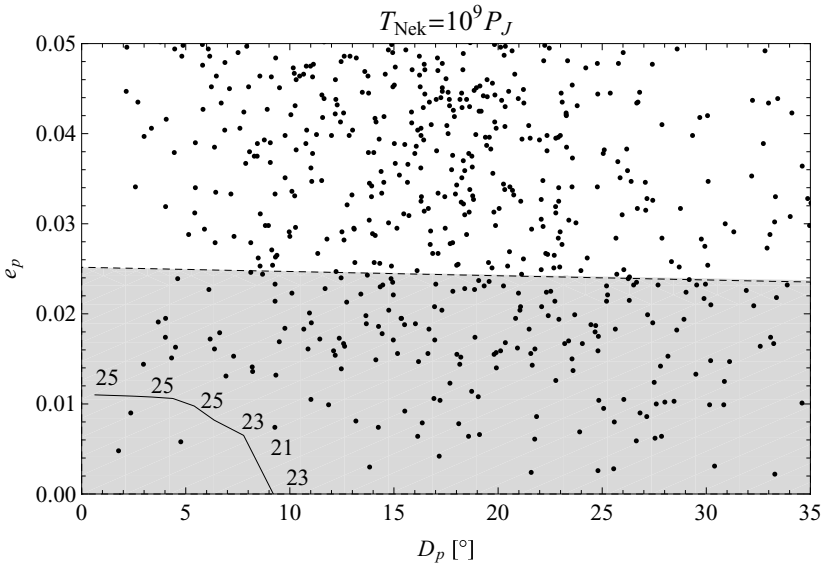

Figure 3. Application of the proposed methods to the case of Jupiters Trojan asteroids (points). The asteroid data are given in proper elements (see the text), the dashed line – limiting the grey-shaded region – gives the radius of convergence of the explicit mapping. The Nekhoroshev stable region is bounded by the solid line, the numbers indicate the optimal order of truncation along different directions and indicate the dependency of the stability region on the angle γ.

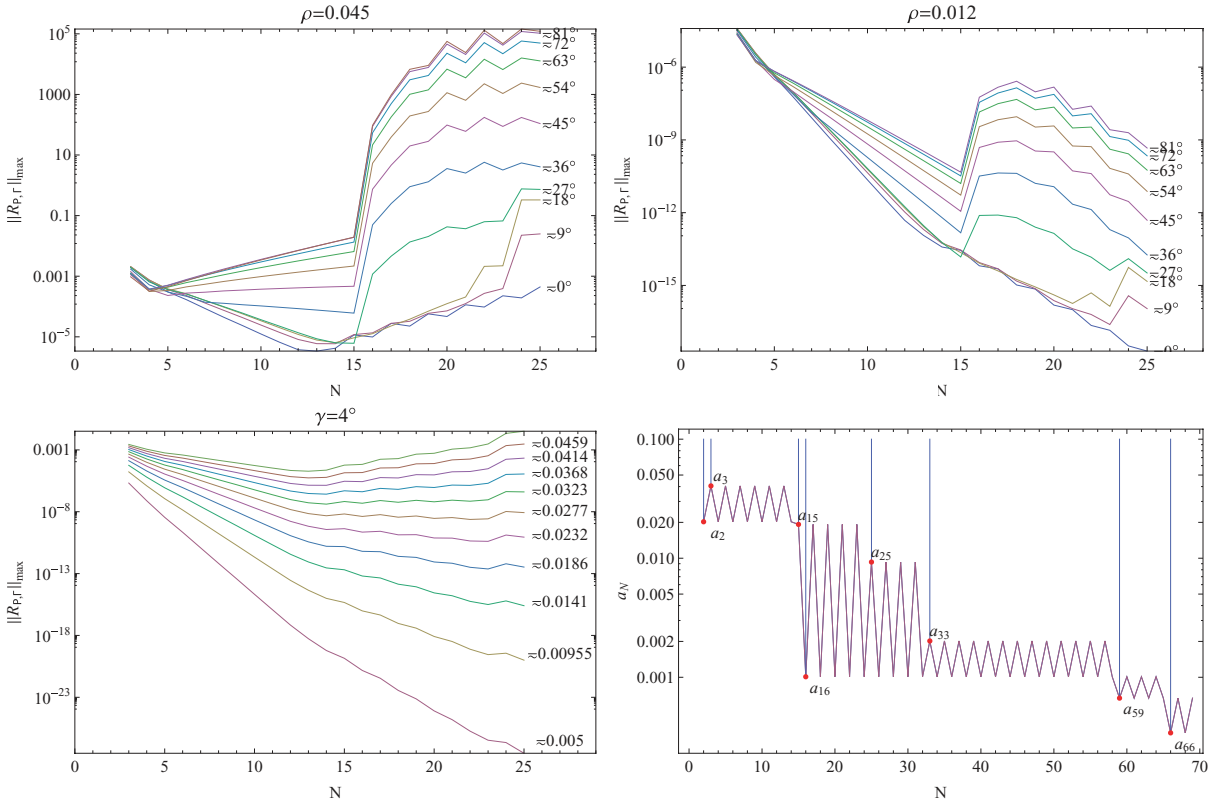

Figure 4. Analysis of the remainder of the series in dependency of the order of truncation N: the size of the remainder max (R_1, R_2) depends on the one hand on γ (for fixed $\rho - 4$a and b), and on the other hand on the distances ρ (for fixed $\gamma - 4$c). With increasing order of normalization, the influence of the small divisors (4d) shows up and changes the behaviour of the remainder of the formal series. The optimal order of truncation turns out to be 23 for small angles in proper element space and increases with increasing γ. This directly influences the Nekhoroshev stable region given in Fig. 3.

is caused by the request to provide a mapping in explicit polynomial form. Thus, after Taylor expansion and reversal, the expanded mapping 'feels' the topological difference in the (ω, e) plane for orbits with free eccentricities below and above $e' = 0.0487$, while this difference does not really introduce resonant effects on the Laplace–Lagrange plane (Fig. 2a).

(ii) The analytically determined domain of Nekhoroshev stability covers a significant domain (about 13 per cent) of the convergence domain. The points show the positions of real asteroids in the (e_p, D_p) plane, following the catalogue http://hamilton.dm.unipi.it/cgi-bin/astdys/astibo, which is based on a variant of Milani's (1993) calculation of proper elements. The comparison is, of course, only indicative, because most asteroids in the catalogue are on inclined orbits, which are also diffusing chaotically towards higher proper eccentricities as a result of resonant interactions with practically the whole outer Solar System (Robutel, Gabern & Jorba 2005). Nevertheless, a few real asteroids are within the analytically calculated domain of stability. This fact shows the physical relevance of the Nekhoroshev like estimator proposed.

Finally, Fig. 4(d) shows the smallest divisors appearing in the series, which cause the asymptotic behavior of the remainder as a function of the normalization order. The main remark here is that the smallest divisor, up to the order of 16, is simply ω_2 indicating that the system is nearly resonant with a second frequency $\omega_2 \simeq 0$. This fact suggests that an improvement of the present estimates can be obtained by the use of adiabatic theory, which, however, is not amenable to the form of the present Birkhoff normalization scheme. On the other hand, the next smaller divisor $a_{16} \simeq 0.001$. appears at $N = 16$, which, according to Figs 4(a)–(c) is close to or beyond the optimal order of normalization for the smallest values of γ. Thus, we have checked that the use of a resonant normal form based on the module $M = \{u_1^{\alpha_1}, v_1^{\beta_1}, u_2^{\alpha_2}, v_2^{\beta_2} : \{\alpha_1, \alpha_2, \beta_1, \beta_2\} \rightarrow a_{16}\}$ does not modify the present estimates appreciably.

5 CONCLUSIONS

We proposed a method yielding analytical estimates of the domain of Nekhoroshev stability around the equilateral points L_4 or L_5 of the planar elliptic restricted three-body model, and implemented it in the case of the Sun–Jupiter–Trojan asteroids configuration. The method is based on deriving an explicit symplectic mapping, via Hadjidemetriou's method, given as a series around a period-one fixed point of the system that corresponds to one of the equilateral Lagrangian points. The analytical apparatus of the Nekhoroshev theory (construction of a Birkhoff normal form, estimates on the size of the remainder) is then used to determine a domain in the space of proper elements (approximate integrals of motion) in which the variations of these elements are bounded over times exceeding the age of the Solar System.

The following are our basic conclusions.

(i) The operations of series expansion and series reversion of the mapping result in a restriction of its domain of convergence. In the case of Jupiter's Trojans, this covers only the librational motions.

(ii) The asymptotic character of the formal series shows up after a particular order called the optimal order of normalization. This order depends on *two* distances in phase space, ρ_1, ρ_2, which roughly correspond to the amplitudes of variation of the libration angle and the eccentricity of the test particle (asteroid), respectively. The size of the series terms containing the smallest divisors, as a function of the overall distance ρ from the equilibrium point, is affected by the direction γ chosen in the plane (ρ_1, ρ_2). This fact is the basis for the derivation of a 2D domain of Nekhoroshev stability in the plane of proper librations versus proper eccentricities.

(iii) Analytical formulae are given relating the size of the domain of stability to the size of the remainder of the normal form series at the optimal order of normalization along a specific direction in (ρ_1, ρ_2).

(iv) In the case of Jupiter's Trojans, the analytically determined domain of Nekhoroshev stability is quite realistic for proper librations ($D_p < 10^0$), and less realistic for proper eccentricities ($e_p < 0.01$). This is partly due to the method itself, which is based on an explicit mapping converging up to $e_p < 0.025$. In addition, the calculation is based on a non-resonant calculation of the Birkhoff normal form, while the frequency of oscillation of the longitude of the perihelion introduces (up to of the order of 16) a near resonance $\omega_2 \simeq 0$. At any rate, the fact that the currently observed values of the proper elements of the asteroids are higher than those allowed by the analytical domain of Nekhoroshev stability in the planar ERTBP may indicate that the chaotic transport along resonances, introduced by the secular variations of Jupiter's elements or by the other planets, has played a major role in determining the present position of the observed asteroids in the space of proper elements.

ACKNOWLEDGMENTS

The work of ChL was fully supported by the FWF (Austrian Science Fund) project P-18930. The authors wish to thank K. Tsiganis and S. Ferraz-Mello for fruitful discussions during the last year.

REFERENCES

Bazzani A., Marmi S., Turchetti G., 1990, Celest. Mech. Dyn. Astron., 47, 333
Bazzani A., Giovannozzi M., Servizi G., Todesco E., Turchetti G., 1993, Physica D, 64, 66
Beaugé C., Roig F., 2001, Icarus, 153, 391
Benettin G., Galgani L., Giorgilli A., 1985, Celest. Mech., 37, 1
Benettin G., Fassò F., Guzzo M., 1998, Regular Chaot. Dyn., 3, 56
Birkhoff G. D., 1920, Acta Math., 43, 1
Brown E. W., Shook C. A., 1964, Planetary Theory. New York, Cambridge University Press, p. 256
Celletti A., Giorgilli A., 1991, Celest. Mech. Dyn. Astron., 50, 31
Efthymiopoulos C., 2005, Celest. Mech. Dyn. Astron., 92, 29
Efthymiopoulos C., Sándor Z., 2005, MNRAS, 364, 253
Efthymiopoulos C., Giorgilli A., Contopoulos G., 2004, J. Phys. A: Math. Gen., 37, 45
Érdi B., 1988, Celest. Mech., 43, 303
Érdi B., 1997, Celest. Mech. Dyn. Astron., 65, 149
Fassó F., Guzzo M., Benettin G., 1998, Commun. Math. Phys., 197, 347
Giorgilli A., 1988, Ann. Inst. H. Poincaré, 48, 423
Giorgilli A., Skokos Ch., 1997, A&A, 317, 254
Giorgilli A., Delshams A., Fontich E., Galgani L., Simó C., 1989, J. Differ. Equ., 77, 167
Guzzo M., Fassó F., Benettin G., 1998, Math. Phys. Electron. J., 4, 1
Hadjidemetriou J. D., 1991, in Roy A. E., ed., Predictability, Stability and Chaos in *N*-Body Dynamical Systems. Plenum Press, New York, p. 157
Hagel J., Lhotka Ch., 2005, Celest. Mechn. Dyn. Astron., 93, 201
Levison H., Shoemaker E. M., Shoemaker C. S., 1997, Nat, 385, 42
Lhotka Ch., 2004,, Univ. Vienna
Littlewood J. E., 1959a, Proc. London Math. Soc., 9, 343
Littlewood J. E., 1959b, Proc. London Math. Soc., 9, 525
Milani A., 1993, Celest. Mech. Dyn. Astron., 57, 59
Nekhoroshev N. N., 1977, Russ. Math. Surv., 32, 1
Robutel P., Gabern F., Jorba A., 2005, Celest. Mech. Dyn. Astron., 92, 53
Stumpff K., 1965, Himmelsmechanik 1, VEB Berlin, p. 288
Sándor Z., Érdi B., 2003, Celest. Mech. Dyn. Astron., 86, 301
Schwarz R., Dvorak R., Suli A., Érdi B., 2007, Astron. Nachr., 328, 785
Servizi G., Turchetti G., Benettin G., Giorgilli A., 1983, Phys. Lett. A, 95, 11
Simó C., 1989, Memorias de la Real Academia de Ciencias y Artes de Barcelona, 48, 303
Skokos Ch., Dokoumetzidis A., 2001, A&A, 367, 729
Tsiganis K., Varvoglis H., Dvorak R., 2005, Celest. Mech. Dyn. Astron., 92, 71
Wolfram Research, Inc., 2005, Mathematica, Version 5.2, Champaign, IL

This paper has been typeset from a TEX/LATEX file prepared by the author.